# Conserved requirement for *EGF–CFC* genes in vertebrate left–right axis formation

**Yu-Ting Yan,[1,3] Kira Gritsman,[2,3] Jixiang Ding,[1] Rebecca D. Burdine,[2] JoMichelle D. Corrales,[2] Sandy M. Price,[1] William S. Talbot,[2] Alexander F. Schier,[2,4] and Michael M. Shen[1,4]**

[1]Center for Advanced Biotechnology and Medicine (CABM) and Department of Pediatrics, University of Medicine and Dentistry of New Jersey–Robert Wood Johnson Medical School, Piscataway, New Jersey 08854 USA; [2]Developmental Genetics Program, Skirball Institute of Biomolecular Medicine, Department of Cell Biology, New York University School of Medicine, New York, New York 10016 USA

**Specification of the left–right (L-R) axis in the vertebrate embryo requires transfer of positional information from the node to the periphery, resulting in asymmetric gene expression in the lateral plate mesoderm. We show that this activation of L-R lateral asymmetry requires the evolutionarily conserved activity of members of the *EGF–CFC* family of extracellular factors. Targeted disruption of murine *Cryptic* results in L-R laterality defects including randomization of abdominal situs, hyposplenia, and pulmonary right isomerism, as well as randomized embryo turning and cardiac looping. Similarly, zebrafish *one-eyed pinhead* (*oep*) mutants that have been rescued partially by mRNA injection display heterotaxia, including randomization of heart looping and pancreas location. In both *Cryptic* and *oep* mutant embryos, L-R asymmetric expression of *Nodal/cyclops*, *Lefty2/antivin*, and *Pitx2* does not occur in the lateral plate mesoderm, while in *Cryptic* mutants *Lefty1* expression is absent from the prospective floor plate. Notably, L-R asymmetric expression of *Nodal* at the lateral edges of the node is still observed in *Cryptic* mutants, indicating that L-R specification has occurred in the node but not the lateral plate. Combined with the previous finding that *oep* is required for *nodal* signaling in zebrafish, we propose that a signaling pathway mediated by *Nodal* and *EGF–CFC* activities is essential for transfer of L-R positional information from the node.**

[Key Words: Left–right asymmetry; isomerism; heterotaxia; node; lateral plate mesoderm; *Nodal*]

Received July 14, 1999; revised version accepted August 13, 1999.

Of the three major body axes, the left–right (L-R) axis is the last to be determined during vertebrate embryogenesis. The initial specification of the L-R axis is likely to begin during late stages of gastrulation, but tissue-specific manifestations of morphological L-R asymmetry become apparent much later in development, throughout organogenesis into the late fetal period (for review, see Ramsdell and Yost 1998; Beddington and Robertson 1999). In all vertebrates, the first overt appearance of L-R asymmetry occurs during early somitogenesis, with an initial rightward bending of the linear heart tube that presages the direction of cardiac looping. In the mouse, another early sign of laterality is the direction of embryonic turning that inverts the three primary germ layers of the embryo. Most morphological L-R asymmetry arises at later stages of organogenesis, when unilateral tissues such as the stomach are positioned on one side, or when bilateral paired tissues such as the lung form asymmetrically. Defects in this process of L-R specification can lead to highly pleiotropic effects, including L-R reversals of organ position (inverted situs), mirror image symmetry of bilaterally asymmetric tissues (isomerism), and/or random and independent occurrence of laterality defects in different tissues (heterotaxia).

Recent molecular genetic studies performed in chick, frog, zebrafish, and mouse systems have shown that tissue-specific laterality decisions are mediated by a pathway of regulatory genes that acts during gastrulation and early postgastrulation stages of embryogenesis. These studies have led to a conceptual pathway for L-R axis determination, in which an initial event that breaks L-R symmetry is believed to occur in or around the embryonic node and its derivatives. The resulting L-R positional information is transferred outward to the lateral plate mesoderm, where it is interpreted to generate the situs of individual tissues (for review, see Harvey 1998; Ramsdell and Yost 1998; Beddington and Robertson 1999; King and Brown 1999). Notably, several members of this regulatory pathway are themselves expressed in a

**[3]These authors contributed equally to this work.**
**[4]Corresponding authors.**
**E-MAIL schier@saturn.med.nyu.edu; FAX (212) 263-7760.**
**E-MAIL mshen@cabm.rutgers.edu; FAX (732) 235-5318.**

L-R asymmetric pattern on the left side of the embryo, in particular the left lateral plate mesoderm.

Several genes in the L-R pathway have roles that appear evolutionarily conserved among vertebrates, including *Nodal* (Levin et al. 1995; Collignon et al. 1996; Lowe et al. 1996; Lustig et al. 1996; Lohr et al. 1997; Sampath et al. 1997; Rebagliati et al. 1998) and *Lefty2* (Meno et al. 1996,1997; Bisgrove et al. 1999; Thisse and Thisse 1999), which encode distant members of the transforming growth factorβ (TGF-β) superfamily, and are asymmetrically expressed in the left lateral plate mesoderm. Another conserved asymmetrically expressed gene is the *Pitx2* homeobox gene, which has been proposed to represent a primary regulator of tissue-specific L-R laterality because it is expressed on the left side of many tissues (Logan et al. 1998; Piedra et al. 1998; Ryan et al. 1998; Yoshioka et al. 1998; Campione et al. 1999). In contrast, there are several apparent differences between vertebrate systems that have complicated our understanding of the L-R pathway. For example, many genes that display transient asymmetry of expression in the chick are not asymmetrically expressed in the mouse, including *activin βB, activin receptor IIA*, and *Sonic hedgehog* (*shh*) (Harvey 1998; Ramsdell and Yost 1998; Beddington and Robertson 1999).

We show that L-R axis formation requires the evolutionarily conserved activity of members of the *EGF–CFC* gene family. The *EGF–CFC* family is comprised of mammalian *Cryptic* and *Cripto*, frog *FRL-1*, and zebrafish *one-eyed pinhead* (*oep*) and encodes extracellular proteins containing a divergent EGF-like motif and a novel cysteine-rich CFC motif (Shen et al. 1997; Zhang et al. 1998). We find that targeted disruption of mouse *Cryptic* results in L-R laterality defects including randomization of abdominal situs, pulmonary right isomerism, and vascular heterotaxia, as well as randomized embryo turning and cardiac looping. In parallel studies, we show that partial rescue of *oep* mutant embryos by *oep* mRNA injection results in randomization of the direction of heart looping and location of the pancreas, revealing that loss of *oep* function leads to heterotaxia. Notably, in both *Cryptic* and *oep* mutant embryos, L-R asymmetric gene expression does not occur in the lateral plate mesoderm. Based on recent studies indicating that EGF–CFC proteins act as essential cofactors for Nodal (Gritsman et al. 1999), we propose that a signaling pathway mediated by Nodal and EGF–CFC proteins is required for activation of L-R asymmetric gene expression in the lateral plate mesoderm.

## Results

### *Targeted disruption of* Cryptic

Previous mutational analyses have revealed that *oep* and *Cripto* have essential requirements prior to gastrulation (Schier et al. 1997; Ding et al. 1998; Gritsman et al. 1999), but it has been unclear if the later expression of *EGF–CFC* genes reflects a role in postgastrulation processes. In particular, *oep* is expressed in the lateral plate mesoderm and forebrain during early somitogenesis (Zhang et al. 1998), and *Cryptic* is expressed in the lateral plate mesoderm, node, notochordal plate, and prospective floor plate from head-fold stages through approximately the six to eight somite stage (Shen et al. 1997). The expression of *oep* and *Cryptic* is symmetric in the lateral plate and precedes the asymmetric expression of genes such as *Nodal/cyclops*, *Lefty2/antivin* and *Pitx2*.

To determine the biological function of *Cryptic*, we performed targeted gene disruption. The *Cryptic* targeting construct should result in a null mutation, because it deleted most of the third exon and the entire fourth and fifth exons of the gene, which encode two-thirds of the mature protein including the central EGF and CFC motifs (Fig. 1a–c). In addition, a second targeting construct that deleted the entire *Cryptic* coding region resulted in the identical homozygous mutant phenotype (Y.-T. Yan, S.M. Price, and M.M. Shen, unpubl.). Homozygosity for the targeted *Cryptic* mutation resulted in neonatal lethality in the first 2 weeks after birth, apparently because of cardiac defects (see below); to date, only five homozygotes (from >90) have survived past weaning. Our initial indication of a phenotypic defect in L-R laterality was that many newborn *Cryptic* homozygotes displayed a milk spot (corresponding to the stomach) on their right side, instead of the left (Fig. 1d).

### *L-R laterality defects in* Cryptic *mutant mice*

To examine the L-R laterality defects of *Cryptic* homozygous mutant mice, we analyzed their gross anatomy at 18.5 days post coitum (dpc) and at neonatal stages (P0–P7) (Table 1). We found that *Cryptic* homozygotes displayed numerous laterality defects, including heterotaxia, randomization of organ situs, and isomerism of bilaterally asymmetric tissues. Thus, within the abdominal cavity, approximately half of the homozygotes ($n$ = 22/49) displayed inverted situs of visceral organs including the stomach, spleen, and pancreas (Fig. 2a,b). In contrast, all homozygous animals displayed asplenia or severe hyposplenia (Fig. 2c–e); a significant proportion of homozygotes also displayed abnormal lobation or midline positioning of the liver (Table 1).

In the thoracic cavity, we found that all homozygotes showed right pulmonary isomerism (Fig. 2f,g); this phenotype is correlated frequently with hyposplenia in human patients with laterality defects (Kosaki and Casey 1998). Moreover, approximately half of the homozygotes ($n$ = 24/50) displayed dextrocardia (cardiac apex pointing to the right) or mesocardia (pointing to the middle), as opposed to the normal levocardia (Fig. 2h–j). Regardless of cardiac situs, nearly all homozygotes displayed cardiac abnormalities, most notably transposition of the great arteries (Fig. 2k,l), as well as severe atrial septal defects (Fig. 2m–o). Finally, we observed numerous random and uncorrelated laterality defects within the vasculature, consistent with heterotaxia (Table 1). For example, the azygos vein could be located on the left side (as it is in the wild type), on the right, or bilaterally (Fig. 2p–r).

The L-R laterality defects observed in neonatal *Cryptic*

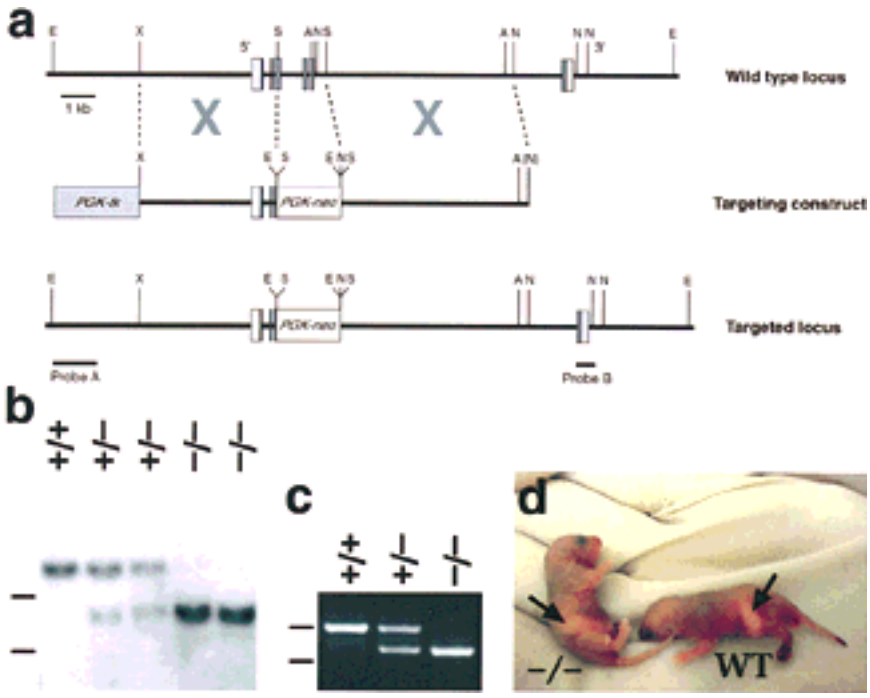


**Figure 1.** Targeted disruption of *Cryptic*. (*a*) Homologous recombination with the targeting vector results in deletion of exons 4 and 5, as well as most of exon 3; exons are shown as boxes, with the coding region in dark gray. (A) *Avr*II; (E) *Eco*RI; (N) *Nhe*I; (S) *Sma*I; (X) *Xba*I. (*b*) Southern blotting using the 5′-flanking probe. A detects an 18-kb *Eco*RI fragment from the wild-type genomic locus and an 8.5-kb fragment from the targeted allele in progeny of $F_1$ heterozygous intercrosses; dashes (*left*) indicate positions of markers at 5 and 10 kb. (*c*) PCR analysis of visceral yolk sac DNA from 7.5-dpc embryos, showing amplification of an 860-bp band corresponding to *Cryptic* and a 735-bp fragment corresponding to *neo*; markers at 615 and 861 bp are indicated as above. (*d*) Neonatal mice with milk spots on the right side (–/–) and left side (WT).

homozygotes were paralleled by phenotypic defects observed in early embryogenesis. At 8.5–9.5 dpc, *Cryptic* homozygous embryos were indistinguishable from their wild-type littermates except for randomization of cardiac looping and embryo turning ($n = 21/45$), with these two phenotypes highly correlated (Fig. 2s–u). Because *Cryptic* is expressed in the notochordal plate and prospective floor plate, and laterality defects are frequently associated with node and notochord defects (e.g., Danos and Yost 1996; Dufort et al. 1998; King et al. 1998; Melloy et al. 1998), we investigated potential axial midline defects by skeletal staining of homozygous neonates ($n = 6$), histological sections at 10.5 dpc ($n = 3$), and in situ hybridization with *Shh*, followed by sectioning ($n = 3$). No evidence for axial midline defects was observed (data not shown).

### *Absence of lateral L-R asymmetric gene expression in* Cryptic *mutant embryos*

To determine the basis for L-R patterning defects in *Cryptic* mutants, we performed in situ hybridization on gastrulation and early somite-stage embryos (up to 10 somites), using probes for *Nodal, Lefty1, Lefty2*, and *Pitx2*, which are asymmetrically expressed at these stages. First, we examined expression of *Lefty1* and *Lefty2*, which are asymmetrically expressed at 2–10 somites in the left prospective floor plate and left lateral plate mesoderm, respectively (Meno et al. 1997, 1998)(Fig. 3a,b,e,f). We found that *Cryptic* homozygous embryos lacked all expression of *Lefty1* ($n = 12$) and *Lefty2* ($n = 9$) at these stages (Fig. 3c,d,g,h); however, an earlier phase of symmetric *Lefty2* expression in newly formed mesoderm during primitive streak stages was un-

**Table 1.** *Phenotype of* Cryptic *homozygous mice*

| Phenotype | Number of mutant/total (%) |
|---|---|
| *Abdominal tissues* | |
| Visceral situs | 22/49 inverted (45%) |
| Spleen | 49/49 asplenic/hyposplenic (100%) |
| Liver | 11/27 abnormal (41%) |
| *Abdominal vasculature* | |
| Branching of inferior vena cava | 16/25 abnormal (64%) |
| Position of renal veins | 4/19 left anterior (21%) |
| *Thoracic tissues* | |
| Cardiac apex | 18/50 dextrocardia, 6/50 mesocardia (48%) |
| Cardiac malformation | 14/16 septal defects (88%); 11/11 transposition of great arteries (100%) |
| Atrial shape | 23/34 right isomerism, 1/34 left (71%) |
| Lung bronchi | 50/50 bilateral eparterial (100%) |
| Lung lobes | 50/50 right isomerism (100%) |
| *Thoracic vasculature* | |
| Aorta relative to pulmonary artery | 44/50 aorta ventral, 5/50 adjacent (98%) |
| Aortic arching | 12/29 right (41%) |
| Position of azygos vein | 5/30 right, 6/30 bilateral (37%) |
| Position of inferior vena cava | 4/33 left, 19/33 bilateral (70%) |

Phenotypes were scored in mice at 18.5 dpc ($n = 6$) and in neonates at <1 week of age ($n = 44$). Not all phenotypes were scored in each mouse. Unless indicated otherwise in the text, the occurrences of these phenotypes were not noticeably correlated with each other.

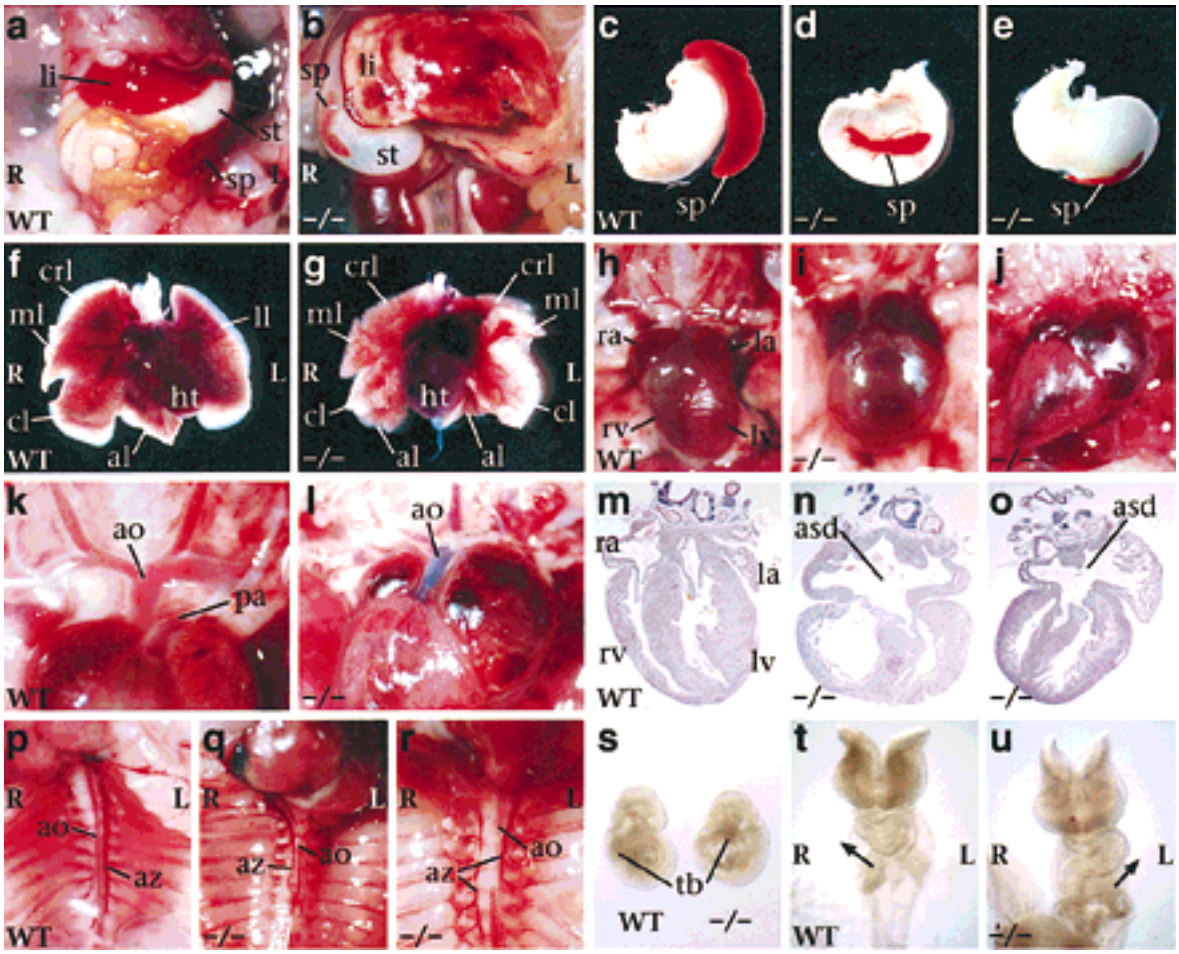


**Figure 2.** L-R laterality defects in *Cryptic* null mutants. (*a–r*) Ventral views of neonatal mice; in all panels, *left* (*L*) and *right* (*R*) are as indicated. Abdominal cavity of wild type (*a*) and mutant (*b*) with inverted situs and hyposplenia. Stomach and spleen from wild type (*c*), mutant with normal situs (*d*), and mutant with inverted abdominal situs (*e*). Heart and lung lobes of wild type (*f*) and mutant (*g*) with right pulmonary isomerism. Heart positions of wild type with normal levocardia (*h*), and mutants with mesocardia (*i*) and dextrocardia (*j*); note correlation with altered size of the atrial chambers. High-power view of cardiac arterial relationships. In the wild type (*k*), the aorta is dorsal to the pulmonary artery and connects to the left ventricle; in the mutant (*l*), the aorta is ventral and connects to the right ventricle, as shown following injection of blue dye into the right ventricle, consistent with transposition of the great arteries. Sections through hearts of wild type (*m*), and two mutants (*n*,*o*) that show an atrial septal defect. Position of the azygos vein and direction of aortic arching. In the wild type (*p*), the azygos vein is located on the *left*, and the aorta arches leftward; in the mutant (*q*), the azygos vein crosses over to the *right* and the aorta arches rightward; in the mutant (*r*), there is a bilateral azygos vein while the aorta arches leftward. (*s*) Lateral views of 8.5-dpc embryos, showing altered direction of embryo turning in the mutant. (*t*,*u*) Ventral views of 10-somite-stage embryos, with arrows indicating direction of cardiac looping in the wild type (*t*) and *Cryptic* mutant (*u*). (al) accessory lobe; (ao) aorta; (asd) atrial septal defect; (az) azygos vein; (cl) caudal lobe; (crl) cranial lobe; (ht) heart; (la) left atrium; (li) liver; (ll) left lung; (lv) left ventricle; (ml) medial lobe; (pa) pulmonary artery; (ra) right atrium; (rv) right ventricle; (sp) spleen; (st) stomach; (tb) tailbud.

affected (data not shown). Next, we examined expression of the homeobox gene *Pitx2*, which is found symmetrically in Rathke's pouch and asymmetrically in the left lateral plate mesoderm and left foregut endoderm from six to eight somites continuing through 9.5 dpc (Ryan et al. 1998; Yoshioka et al. 1998) (Fig. 3i,j). In *Cryptic* mutants at 8.5 and 9.5 dpc ($n = 16$), *Pitx2* expression was still observed in Rathke's pouch but not in the asymmetric domains (Fig. 3k,l).

Finally, we examined expression of *Nodal*, which is found at the lateral boundaries of the node at head-fold and early somite stages, with a transient phase of L-R asymmetry at four to eight somites, and in the left lateral plate mesoderm at approximately two to eight somites (Collignon et al. 1996; Lowe et al. 1996) (Fig. 3m,n). In *Cryptic* mutants ($n = 41$), *Nodal* expression was observed at the lateral boundaries of the node but was never detected in the lateral plate mesoderm (Fig. 3o,p). Notably, the markedly asymmetric expression of *Nodal* at the edges of the node at four to eight somites was still observed in the *Cryptic* mutant embryos ($n = 29$; Fig. 3q–s). Thus, our in situ hybridization results indicate that L-R

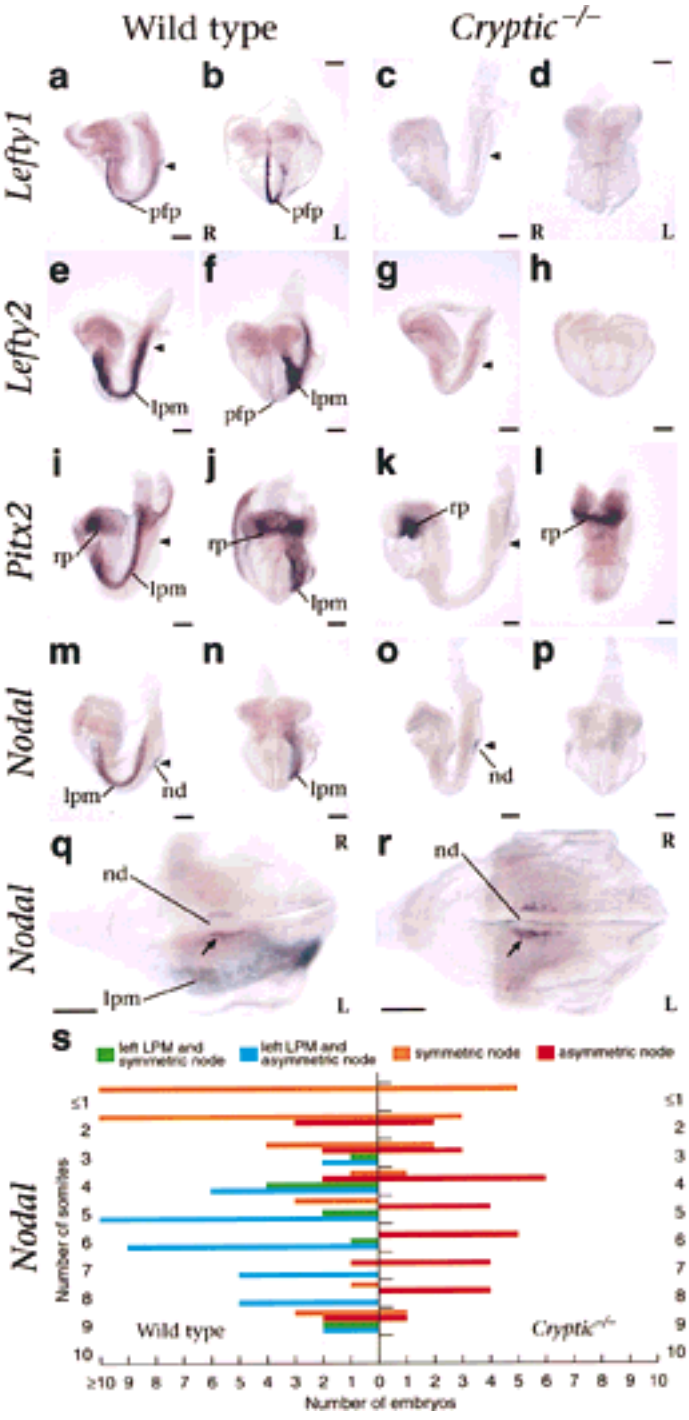


**Figure 3.** Expression of L-R pathway genes in *Cryptic* homozygous mutant embryos. (*a–p*) Lateral and frontal views of early somite stage mouse embryos following whole-mount in situ hybridization. *Left* (*L*) and *right* (*R*) are as shown, and the position of the node is indicated by an arrowhead. Expression of *Lefty1* is detected in the prospective floor plate of wild type (*a*,*b*) but not mutant embryos (*c*,*d*). Expression of *Lefty2* is detected in the left lateral plate mesoderm and weakly in the prospective floor plate of wild type (*e*,*f*) but not *Cryptic* homozygotes (*g*,*h*). *Pitx2* expression is observed symmetrically in Rathke's pouch in both wild type (*I*,*j*) and mutant (*k*,*l*) embryos, but asymmetric expression in the left lateral plate mesoderm is observed only in the wild type. *Nodal* expression is detected in the node of both wild-type (*m*,*n*) and mutant (*o*,*p*) embryos; left lateral plate expression is observed only in the wild type. High-power caudal views of the node in wild-type (*q*) and *Cryptic* homozygote (*r*) show asymmetric expression of *Nodal*. (*s*) Graphical representation of *Nodal* in situ hybridization results. The numbers of wild-type and *Cryptic* mutant embryos analyzed with the indicated *Nodal* expression patterns are graphed according to somite stage. (lpm) lateral plate mesoderm; (nd) node; (pfp) prospective floor plate; (rp) Rathke's pouch.

laterality has been initiated within the node but not in the lateral plate mesoderm.

### *Heterotaxia in* oep *mutant fish*

To determine if the function of *EGF–CFC* genes in L-R determination is conserved in vertebrates, we studied the role of the zebrafish *oep* gene. Previous studies have shown that *oep* is required for formation of mesoderm, endoderm, prechordal plate, and ventral neuroectoderm, correlating with the expression of *oep* in the progenitors of these cell types (Schier et al. 1997; Zhang et al. 1998; Gritsman et al. 1999). During somitogenesis, *oep* is also expressed in the left and right lateral plate, where progenitors of the heart and other organs are located in wild-type embryos (Serbedzija et al. 1998; Zhang et al. 1998). The potential role of *oep* in these territories cannot be analyzed in *oep* mutants, because mutant embryos lack

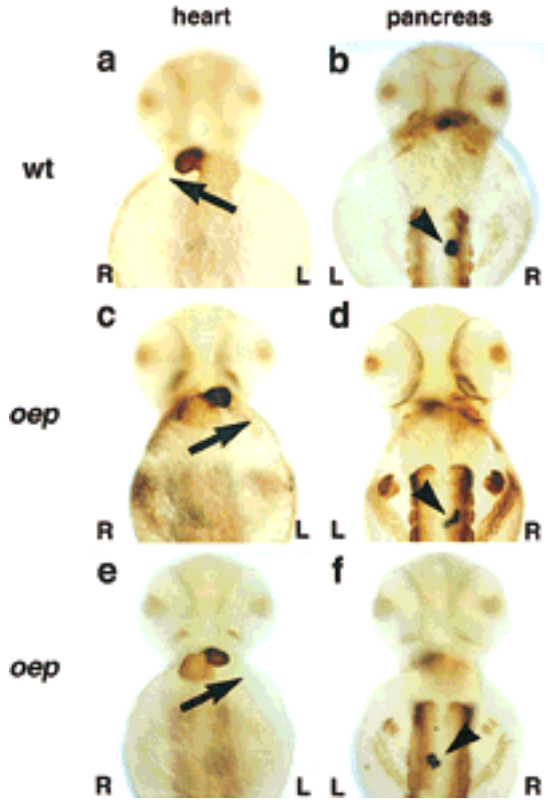


**Figure 4.** Heart looping and location of the pancreas in *oep* mutants. Ventral (*a*,*c*,*e*) and dorsal views (*b*,*d*,*f*) of embryos upon immunohistochemistry with MF20 antibody (Bader et al. 1982) and RNA in situ hybridization with *insulin* probe (Milewski et al. 1998); anterior is up. (*a*,*b*) Wild-type embryo; (*c*,*d* and *e*,*f*) two examples of maternal-zygotic *oep* mutant embryos rescued by injection of *oep* mRNA. Note the normal development of eyes and trunk muscle (*d*,*f*) in rescued embryos [maternal–zygotic *oep* mutants show cyclopia and absence of trunk muscle (Gritsman et al. 1999)]. The arrow indicates heart looping from the atrium (weaker staining, posteriorly) to the ventricle (stronger staining, anteriorly); note right looping in *a* and left looping in *c* and *e*. The arrowhead indicates position of pancreas on *right* (*b*,*d*) or *left* (*f*) side. We note that the direction of cardiac looping in rescued mutants did not significantly affect their survival to adulthood [50/70 (71%) of right-looping embryos, 46/53 (87%) of left-looping embryos, and 2/6 (33%) of nonlooping embryos survived].

endodermal derivatives and heart (Schier et al. 1997; Gritsman et al. 1999). To circumvent this limitation, we examined the phenotype of maternal–zygotic *oep* (MZ*oep*) embryos whose early defects were rescued by *oep* mRNA injection (Fig. 4). Injected mRNA is present throughout gastrulation (data not shown) and is sufficient to completely rescue the formation of endoderm, mesoderm, axial midline, and ventral neuroectoderm (Fig. 4c–f), but is apparently insufficient to complement the loss of *oep* activity at later stages. Using morphological criteria and marker gene expression, we found that heart and pancreas form, but that the direction of heart looping and the location of the pancreas are randomized with respect to the L-R axis of the embryo (Fig. 4c–f; Table 2). More than 81% (48/59) of *oep* mutant embryos that display abnormal heart asymmetry during embryogenesis survive to adulthood, demonstrating that mRNA injection rescues the development and function of all essential organs. Notably, there was no correlation between abnormal heart asymmetry and the location of the pancreas, revealing that loss of *oep* function leads to heterotaxia.

### *Absence of L-R asymmetric gene expression in* oep *mutants*

To determine the onset of the L-R patterning defect in *oep* mutants, we performed in situ hybridization on somite-stage embryos using probes for *cyclops*, *antivin* (a member of the *lefty* family), and *pitx2*, which are all asymmetrically expressed in the lateral plate mesoderm (Rebagliati et al. 1998; Campione et al. 1999; Thisse and Thisse 1999). Analogous to *Cryptic* mouse mutants, we never detected the normal asymmetric expression of these markers, despite wild-type expression in other regions of the embryo (Fig. 5) . Importantly, asymmetric expression is not initiated, revealing a role for *oep* in the induction of lateral plate asymmetry.

## Discussion

Our comparative mutational analyses have shown that homozygous *Cryptic* null mutant mice and partially res-

**Table 2.** *Direction of heart looping and location of pancreas in wild-type and* oep *mutants*

Genotype: *oep*/+ (+/+ female × –/– male)
Injected mRNA: *lacZ*
Total no. embryos: 96

| | | Heart (MF20) | | |
|---|---|---|---|---|
| Pancreas (insulin) | | L | M | R |
| R | 83 (86.5%) | 2 (2.1%) | 0 | 81 (84.3%) |
| M | 6 (6.2%) | 0 | 4 (4.2%) | 2 (2.1%) |
| L | 7 (7.3%) | 4 (4.2%) | 0 | 3 (3.1%) |

Genotype: *oep*/+ (+/+ female × –/– male)
Injected mRNA: *oep*
Total no. embryos: 108

| | | Heart (MF20) | | |
|---|---|---|---|---|
| Pancreas (insulin) | | L | M | R |
| R | 90 (83.3%) | 6 (5.5%) | 3 (2.8%) | 81 (75.0%) |
| M | 4 (3.7%) | 2 (1.9%) | 0 | 2 (1.9%) |
| L | 14 (13.0%) | 9 (8.3%) | 0 | 5 (4.6%) |

Genotype: *oep*/*oep* (–/– female × –/– male)
Injected mRNA: *oep*
Total no. embryos: 106

| | | Heart (MF20) | | |
|---|---|---|---|---|
| Pancreas (insulin) | | L | M | R |
| R | 48 (45.3%) | 20 (18.9%) | 1 (0.9%) | 27 (25.5%) |
| M | 7 (6.6%) | 2 (1.9%) | 1 (0.9%) | 4 (3.8%) |
| L | 51 (48.1%) | 26 (24.5%) | 1 (0.9%) | 24 (22.7%) |

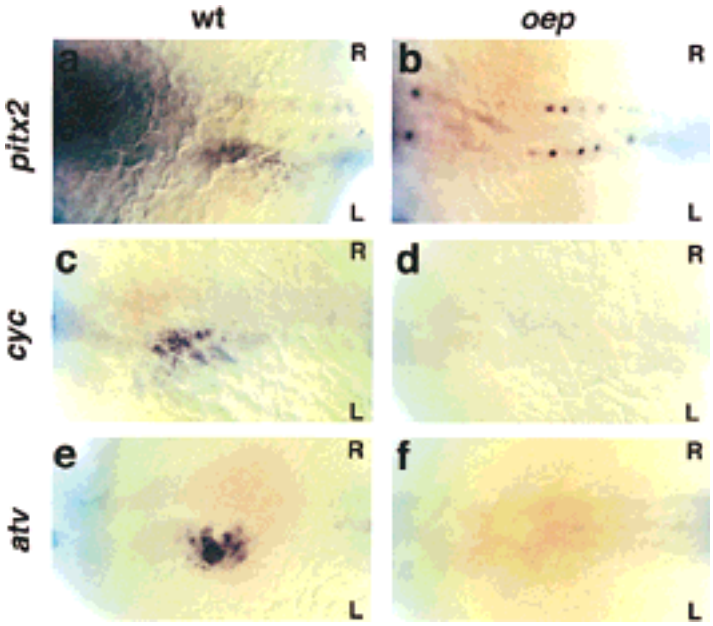


**Figure 5.** Expression of L-R pathway genes in *oep* mutant embryos. Dorsal view (anterior to the *left*) of 22-somite-stage (*a–d*) and 24-somite-stage (*e,f*) embryos following whole-mount in situ hybridization with *pitx2* (*a,b*), *cyclops* (*c,d*), or *antivin* (*e,f*). Normal expression in the left lateral plate is only detected in wild-type (*a,c*, *oep*/+ embryo injected with *oep* mRNA; *e*, *oep*/+ embryo injected with *lacZ* mRNA) but not in maternal–zygotic *oep* mutants whose early patterning defects were rescued by *oep* mRNA injection (*b*, *n* = 58 embryos analyzed between 14- and 24-somite stages; *d*, *n* = 67; *f*, *n* = 44). Note the normal expression of *pitx2* in the spinal cord (*b*).

cued *oep* mutant fish both display highly penetrant L-R heterotaxia defects. Notably, in *Cryptic* as well as *oep* mutant embryos, *Nodal, Lefty2/antivin*, and *Pitx2* are not expressed in the lateral plate mesoderm, indicating that *EGF–CFC* activity is essential for asymmetric gene expression in the lateral mesoderm. Taken together, our findings with *oep* mutant fish are analogous to those for *Cryptic* mutant mice, and establish an evolutionarily conserved requirement for *EGF–CFC* genes in the establishment of L-R asymmetry in vertebrates. Interestingly, this evolutionary conservation of *EGF–CFC* activity in the L-R pathway markedly contrasts with the apparent non-conserved roles of *Fgf8* and *Shh* in the mouse and chick (Meyers and Martin 1999).

### *Essential function of* EGF–CFC *genes in L-R axis specification*

Our results can be readily integrated with a general pathway for L-R axis determination in which initial L-R symmetry is broken in or around the node, and subsequent L-R positional information is transferred to the lateral plate mesoderm (Levin et al. 1995; Logan et al. 1998; Pagan-Westphal and Tabin 1998; Beddington and Robertson 1999). Given the requirement of *oep* activity for *nodal* signaling in zebrafish and the functional conservation of EGF–CFC proteins (Gritsman et al. 1999), we propose that *Cryptic* and *oep* are essential for *Nodal* signaling in L-R axis specification. Our findings indicate that *EGF–CFC* activity is required prior to the activation of L-R asymmetric gene expression in the periphery and may be involved in events downstream from an initial process that breaks L-R symmetry.

Specifically, our results are consistent with two possible models for *EGF–CFC* function in L-R axis formation (Fig. 6). In the first model, *Cryptic/oep* would be required in the lateral plate mesoderm to mediate the response to an asymmetric 'left'-determining signal emanating from the node (Fig. 6a,b). This signal might correspond to Nodal itself, as we have shown previously that EGF–CFC proteins are required for cells to respond to Nodal signals (Gritsman et al. 1999). In this scenario, Nodal signaling from the node or its derivatives cannot be received due to the absence of EGF–CFC activity in the lateral plate.

In the second model for *EGF–CFC* function, *Cryptic/oep* would be required at an earlier stage in the node or its derivatives for the generation or propagation of an asymmetric signal, which could either correspond to Nodal itself or be dependent on Nodal signaling (Fig. 6c). Defects in axial midline structures often result in L-R laterality defects and alterations in asymmetric gene expression, as seen for mouse mutations in *no turning*, *HNF-3β, Brachyury,* and *SIL* (Dufort et al. 1998; King et al. 1998; Melloy et al. 1998; Izraeli et al. 1999) and for zebrafish mutations in *no tail* or *floating head* (Danos and Yost 1996; Chen et al. 1997). Although there are no apparent structural defects in the node or its derivatives in *Cryptic* and partially rescued *oep* mutants, absence of EGF–CFC activity might result in a block in Nodal signaling in the axial midline, indirectly leading to defects in the lateral plate (Fig. 6c). Of course, these models are not mutually exclusive, and *Cryptic/oep* may act in both the node and lateral plate. In either case, *EGF–CFC* activity would play an essential role in transferring L-R positional information from the node to the periphery, resulting in asymmetric *Nodal* and *Lefty2/antivin* expression in the lateral plate mesoderm, asymmetric *Lefty1* expression in the mouse floor plate, and subsequent asymmetric *Pitx2* expression, ultimately leading to specification of individual organ situs.

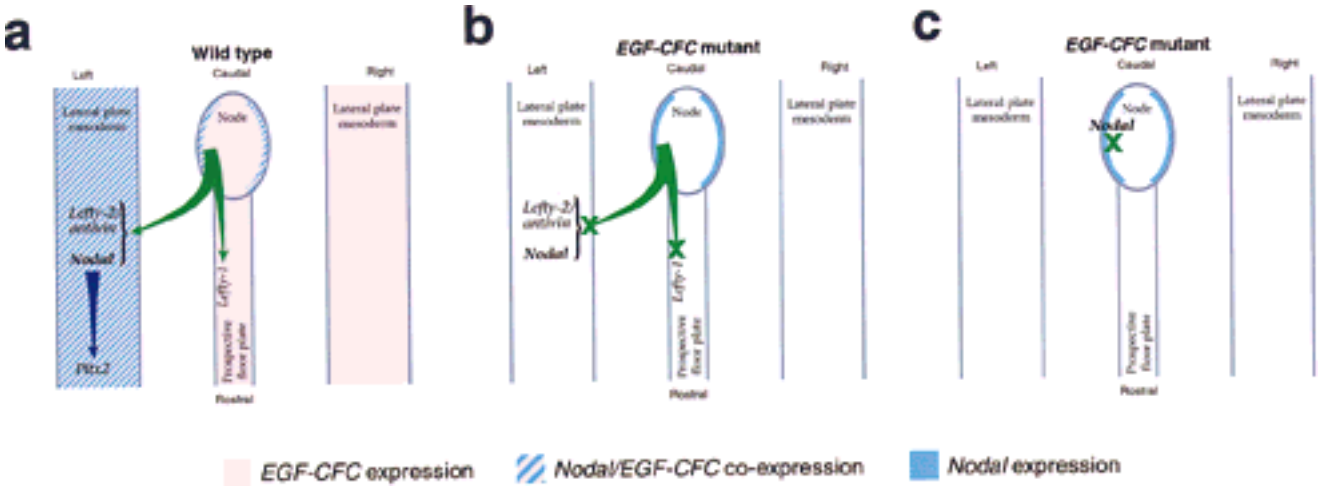


**Figure 6.** Schematic model for *EGF–CFC* function in L-R axis formation. (*a*) In wild-type embryos, a asymmetric signal emanating from the node activates expression of *Nodal/cyclops* and *Lefty2/antivin* in the left lateral plate mesoderm, as well as *Lefty1* in the left prospective floor plate, leading to subsequent activation of *Pitx2* and specification of organ situs. The node-derived signal could correspond to Nodal itself or to a hypothesized factor downstream of *Shh* signaling that conveys L-R positional information in the chick (Pagan-Westphal and Tabin 1998). (*b*) In this model, the response to the asymmetric node-derived signal is mediated by *Cryptic/oep*, which is symmetrically expressed in the lateral plate mesoderm. In the absence of *EGF–CFC* activity, the lateral plate and prospective floor plate do not respond to the node-derived signal, and asymmetric gene expression fails to occur, resulting in subsequent L-R laterality defects. (*c*) Here, *Cryptic/oep* is required to mediate a *Nodal* activity that is downstream of an initial L-R symmetry-breaking event in or around the node. As a consequence, L-R laterality is specified around the node but fails to be propagated to the lateral plate mesoderm.

### Cryptic *mutants as a model for right isomerism/asplenia syndrome*

In humans, the proper L-R situs of the visceral tissues is critical for their morphogenesis and/or physiological function, particularly in the cardiovascular system. In particular, children born with severe heterotaxia generally die shortly after birth, usually due to severe cardiac defects. In many cases, laterality defects in humans that result in heterotaxia can be classified into two primary categories: right isomerism associated with asplenia/hyposplenia and, conversely, left isomerism associated with polysplenia (Goldstein et al. 1998; Kosaki and Casey 1998). Our studies show that *Cryptic* mutant mice recapitulate many features of the right isomerism/asplenia syndrome, suggesting that the *Cryptic* mutant mice may represent a model for a major category of human L-R laterality defects.

### *Interaction of EGF–CFC genes with the Nodal signaling pathway*

In contrast to the phenotype reported here for *oep*, mutations in the zebrafish *nodal* gene *cyclops* do not result in a significant incidence of heart looping defects (Chen et al. 1997). These differing laterality phenotypes of *oep* versus *cyclops* mutants may be due to redundant functions of zebrafish *nodal*-related genes in L-R axis determination. Moreover, a direct requirement for mouse *Nodal* in L-R patterning has also been difficult to establish, due to the early embryonic lethality of *Nodal* mutants, which precludes analysis of later defects. Nonetheless, the L-R phenotypes of *Cryptic* and *oep* mutants, together with the phenotypes of *Nodal*$^{+/-}$; *HNF-3*B$^{+/-}$ and *Nodal*$^{+/-}$; *Smad2*$^{+/-}$ mutants (Collignon et al. 1996; Nomura and Li 1998), strongly suggest that Nodal signals are essential for L-R axis specification.

Although the Nodal signaling pathway has not been analyzed at the biochemical level, loss- and gain-of-function studies in mouse, frog, and fish suggest that during gastrulation Nodal signals may act via activin-like receptors (Hemmati-Brivanlou and Melton 1992; Armes and Smith 1997; Chang et al. 1997; New et al. 1997; Oh and Li 1997; Gu et al. 1998; Gritsman et al. 1999; Meno et al. 1999) and the transcription factor Smad2 (Baker and Harland 1996; Graff et al. 1996; Nomura and Li 1998; Waldrip et al. 1998; Weinstein et al. 1998). During germ-layer formation, Nodal signaling has also been shown to be dependent on EGF–CFC activity (Gritsman et al. 1999) and to be antagonized by members of the *Lefty* family (Bisgrove et al. 1999; Meno et al. 1999; Thisse and Thisse 1999). Therefore, it is thought that during gastrulation, Nodal signals are dependent on EGF–CFC proteins to activate activin-like receptors and Smad2, leading to the induction of *Lefty* genes and the attenuation of Nodal signaling.

Comparison of the L-R phenotypes of *Cryptic* and *oep* mutants with the defects found in *Lefty1* and *ActRIIB* mutant mice extends this model to L-R axis determination, raising the possibility that EGF–CFC proteins act universally as essential cofactors for Nodal signaling. First, mice lacking *Lefty1* (Meno et al. 1998) frequently display left pulmonary isomerism and bilateral expression of *Nodal*, *Lefty2*, and *Pitx2*. In contrast, *Cryptic*

mutants display right pulmonary isomerism and lack asymmetric gene expression in the lateral plate mesoderm. These opposing phenotypes support the notion that *Lefty1* acts by antagonizing EGF–CFC dependent *Nodal* activity during L-R determination. Secondly, the phenotype of *Cryptic* mutants superficially resembles that of *ActRIIB* mutant mice, which display right pulmonary isomerism and severe cardiac defects (Oh and Li 1997). Moreover, although *Smad2* homozygotes display early embryonic lethality due to defective specification of the anteroposterior (AP) axis (Nomura and Li 1998; Waldrip et al. 1998; Weinstein et al. 1998), a significant percentage of *Nodal*$^{+/-}$; *Smad2*$^{+/-}$ compound heterozygotes display L-R laterality defects (Nomura and Li 1998), which are similar to those of *Cryptic* mutants. The greater severity of the laterality defects in *Cryptic* mice relative to those of *ActRIIB* mutants may reflect the ability of Nodal in conjunction with EGF–CFC proteins to signal through a type II receptor that is partially redundant with ActRIIB, perhaps ActRIIA (also known as ActRII). In summary, these findings indicate that Nodal signaling during L-R development is mediated by EGF–CFC proteins, activin receptors, and Smad2.

### *Conservation of EGF–CFC function in embryonic axis formation*

The phenotypes of *Cripto* and *Cryptic* mutations in mice bear remarkable similarity to those of mutant zebrafish with different timing of *oep* activity. Specifically, complete removal of both maternal and zygotic *oep* activity (MZ*oep* mutants) results in loss of head and trunk mesoderm, endoderm, and an incorrectly positioned AP axis (Gritsman et al. 1999), a phenotype similar to that of *Cripto* mutant mice (Ding et al. 1998). Conversely, restoration of early *oep* activity to MZ*oep* embryos by *oep* mRNA injection rescues these defects, but the insufficient persistence of injected mRNA results in a subsequent L-R laterality defect that strongly resembles the phenotype of *Cryptic* mutants. Taken together, our results indicate that a Nodal and EGF–CFC signaling pathway is essential for both the AP and L-R axes in vertebrates, with the dual role for *oep* in both processes in fish being divided between the related genes *Cripto* and *Cryptic* in mice.

## Materials and methods

### *Gene targeting*

A murine *Cryptic* cDNA was used to screen a λFIXII library constructed from 129Sv/J genomic DNA (Stratagene), resulting in the isolation of a 21-kb genomic clone containing the entire coding region. To construct a targeting vector for *Cryptic*, a 3.5-kb *Xba*I–*Sma*I 5′ flank was subcloned into the *Xba*I–*Sma*I sites of *pTKLNL* (Mortensen 1999), followed by subcloning of a 5.0-kb *Sma*I–*Nhe*I 3′ flank, such that the *PGK–neo* and *PGK–tk* cassettes are in the opposite transcriptional orientation to *Cryptic*. Targeting was performed using TC1 ES cells (Deng et al. 1996), with targeted clones obtained at a frequency of 5% (4/88); ES cell culture and blastocyst injection were performed as described previously (Ding et al. 1998). Chimeric males obtained following blastocyst injection were bred with Black Swiss females (Taconic), and germ-line transmission was obtained from one targeted ES clone; two independent lines were also derived using a different targeting vector (Y.-T. Yan, S.M. Price, and M.M. Shen, unpubl.). These targeted *Cryptic* mutations have been maintained through backcrossing with outbred Black Swiss mice; the phenotype appears similar in each line. In addition, the homozygous phenotype appears similar in a hybrid 129/SvEvTac-C57BL/6J strain background.

### *Mouse genotyping and phenotypic analysis*

Genotyping was performed by Southern blotting or by PCR using genomic DNA prepared from tails or embryonic visceral yolk sac. Primers for genotyping were as follows: for wild-type *Cryptic*, 5′GGAGATGGTGCCAGAGAAGTCAGC3′ and 5′AATAGGCAGGGCACACGCAGAAAC3′; for *neo*, 5′CTGCCGCGCTGTTCTCCTCTTCCT3′ and 5′ACACCCAGCCGGCCACAGTCG3′. The presence of cardiac septal defects and transposition of the great arteries was scored by injection of bromphenol blue dye into the right ventricle (Oh and Li 1997), and ventriculoarterial alignment was confirmed by histological sectioning. Cardiac histology was performed by hematoxylin-eosin staining of paraffin sections, with attention given to L-R orientation of sections. Whole-mount in situ hybridization to mouse embryos was performed as described (Ding et al. 1998), using probes for murine *Lefty1* (Meno et al. 1997), *Lefty2* (Meno et al. 1997), *Nodal* (Lowe et al. 1996), and *Pitx2* (Lanctèt et al. 1999).

### *Zebrafish genetics and phenotypic analysis*

Homozygous *oep*$^{tz57}$/*oep*$^{tz57}$ adults were obtained by rescue of homozygous *oep*$^{tz57}$/*oep*$^{tz57}$ embryos with *oep* mRNA (Zhang et al. 1998; Gritsman et al. 1999). To rescue the early patterning defects of *oep* mutants, maternal-zygotic *oep*$^{tz57}$/*oep*$^{tz57}$ embryos were injected with 25–50 pg of *oep* mRNA at the one- to four- cell stage. Heart looping was scored in live embryos and by immunohistochemistry using the MF20 antibody (Bader et al. 1982) that recognizes a myosin heavy chain. Embryos were then processed for in situ hybridization using an *insulin* antisense RNA probe (Milewski et al. 1998). Whole-mount in situ hybridization for *cyclops*, *antivin*, and *Pitx2* was performed as described (Zhang et al. 1998). Zebrafish *pitx2* was cloned by screening of a cDNA library (kindly provided by B. Appel and J. Eisen, University of Oregon, Eugene) with a PCR-amplified *pitx2* homeobox probe (R.D. Burdine; A.F. Schier, and W.S. Talbot, GenBank accession nos. AF156905 and AF156906).

## Acknowledgments

We thank Anukampa Barth, Jacques Drouin, Hiroshi Hamada, Yoshiyuki Imai, Michael Kuehn, Rick Mortensen, Cliff Tabin, Bernard Thisse, Christine Thisse, and Steve Wilson for gifts of probes and reagents. We also thank Nishita Desai, Rory Feeney, Elizabeth Heckscher, and Magdalena Michalski for technical assistance. We are particularly grateful to Cory Abate-Shen, Robert Cardiff, and Cliff Tabin for helpful discussions and comments on the manuscript. This work was supported by postdoctoral fellowships from the American Heart Association (J.D.) and Damon Runyon–Walter Winchell Cancer Research Fund (R.D.B.), and by grants from the National Science Foundation (M.M.S.), the American Heart Association (M.M.S.), the U.S.

Army Breast Cancer Research Program (M.M.S.), and the National Institutes of Health (W.S.T., A.F.S., M.M.S.). A.F.S. is a Scholar of the McKnight Endowment Fund for Neuroscience.

The publication costs of this article were defrayed in part by payment of page charges. This article must therefore be hereby marked 'advertisement' in accordance with 18 USC section 1734 solely to indicate this fact.

## References

Armes, N.A. and J.C. Smith. 1997. The ALK-2 and ALK-4 activin receptors transduce distinct mesoderm-inducing signals during early Xenopus development but do not cooperate to establish thresholds. *Development* **124:** 3797–3804.

Bader, D., T. Masaki, and D.A. Fischman. 1982. Immunochemical analysis of myosin heavy chain during avian myogenesis in vivo and in vitro. *J. Cell Biol.* **95:** 763–770.

Baker, J.C. and R.M. Harland. 1996. A novel mesoderm inducer, Madr2, functions in the activin signal transduction pathway. *Genes & Dev.* **10:** 1880–1889.

Beddington, R.S.P. and E.J. Robertson. 1999. Axis development and early asymmetry in mammals. *Cell* **96:** 195–209.

Bisgrove, B.W., J.J. Essner, and H.J. Yost. 1999. Regulation of midline development by antagonism of *lefty* and *nodal* signaling. *Development* **126:** 3253–3262.

Campione, M., H. Steinbeisser, A. Schweickert, K. Deissler, F. van Bebber, L.A. Lowe, S. Nowotschin, C. Viebahn, P. Haffter, M.R. Kuehn et al. 1999. The homeobox gene *Pitx2*: Mediator of asymmetric left-right signaling in vertebrate heart and gut looping. *Development* **126:** 1225–1234.

Chang, C., P.A. Wilson, L.S. Mathews, and A. Hemmati-Brivanlou. 1997. A Xenopus type I activin receptor mediates mesodermal but not neural specification during embryogenesis. *Development* **124:** 827–837.

Chen, J.N., F.J. van Eeden, K.S. Warren, A. Chin, C. Nusslein-Volhard, P. Haffter, and M.C. Fishman. 1997. Left-right pattern of cardiac BMP4 may drive asymmetry of the heart in zebrafish. *Development* **124:** 4373–4382.

Collignon, J., I. Varlet, and E.J. Robertson. 1996. Relationship between asymmetric *nodal* expression and the direction of embryonic turning. *Nature* **381:** 155–158.

Danos, M.C. and H.J. Yost. 1996. Role of notochord in specification of cardiac left-right orientation in zebrafish and Xenopus. *Dev. Biol.* **177:** 96–103.

Deng, C., A. Wynshaw-Boris, F. Zhou, A. Kuo, and P. Leder. 1996. Fibroblast growth factor receptor 3 is a negative regulator of bone growth. *Cell* **84:** 911–921.

Ding, J., L. Yang, Y.T. Yan, A. Chen, N. Desai, A. Wynshaw-Boris, and M.M. Shen. 1998. *Cripto* is required for correct orientation of the anterior-posterior axis in the mouse embryo. *Nature* **395:** 702–707.

Dufort, D., L. Schwartz, K. Harpal, and J. Rossant. 1998. The transcription factor HNF3beta is required in visceral endoderm for normal primitive streak morphogenesis. *Development* **125:** 3015–3025.

Goldstein, A.M., B.S. Ticho, and M.C. Fishman. 1998. Patterning the heart's left-right axis: From zebrafish to man. *Dev. Genet.* **22:** 278–287.

Graff, J.M., A. Bansal, and D.A. Melton. 1996. Xenopus Mad proteins transduce distinct subsets of signals for the TGF beta superfamily. *Cell* **85:** 479–487.

Gritsman, K., J. Zhang, S. Cheng, E. Heckscher, W.S. Talbot, and A.F. Schier. 1999. The EGF–CFC protein one-eyed pinhead is essential for nodal signaling. *Cell* **97:** 121–132.

Gu, Z., M. Nomura, B.B. Simpson, H. Lei, A. Feijen, J. van den Eijnden-van Raaij, P.K. Donahoe, and E. Li. 1998. The type I activin receptor ActRIB is required for egg cylinder organization and gastrulation in the mouse. *Genes & Dev.* **12:** 844–857.

Harvey, R.P. 1998. Links in the left/right axial pathway. *Cell* **94:** 273–276.

Hemmati-Brivanlou, A. and D.A. Melton. 1992. A truncated activin receptor inhibits mesoderm induction and formation of axial structures in Xenopus embryos. *Nature* **359:** 609–614.

Izraeli, S., L.A. Lowe, V.L. Bertness, D.J. Good, D.W. Dorward, I.L. Kirsch, and M.R. Kuehn. 1999. The *SIL* gene is required for mouse embryonic axial development and left-right specification. *Nature* **399:** 691–694.

King, T., R.S.P. Beddington, and N.A. Brown. 1998. The role of the *brachyury* gene in heart development and left-right axis specification in the mouse. *Mech. Dev.* **79:** 29–37.

King, T. and N.A. Brown. 1999. Embryonic asymmetry: The left side gets all the best genes. *Curr. Biol.* **9:** R18–R22.

Kosaki, K. and B. Casey. 1998. Genetics of human left-right axis malformations. *Sem. Cell Dev. Biol.* **9:** 89-99.

Lanctèt, C., A. Moreau, M. Chamberland, M.L. Tremblay, and J. Drouin. 1999. Hindlimb patterning and mandible development require the Ptx1 gene. *Development* **126:** 1805–1810.

Levin, M., R.L. Johnson, C.D. Stern, M. Kuehn, and C. Tabin. 1995. A molecular pathway determining left-right asymmetry in chick embryogenesis. *Cell* **82:** 803–814.

Logan, M., S.M. Pagan-Westphal, D.M. Smith, L. Paganessi, and C.J. Tabin. 1998. The transcription factor Pitx2 mediates situs-specific morphogenesis in response to left-right asymmetric signals. *Cell* **94:** 307–317.

Lohr, J.L., M.C. Danos, and H.J. Yost. 1997. Left-right asymmetry of a nodal-related gene is regulated by dorsoanterior midline structures during Xenopus development. *Development* **124:** 1465–1472.

Lowe, L.A., D.M. Supp, K. Sampath, T. Yokoyama, C.V. Wright, S.S. Potter, P. Overbeek, and M.R. Kuehn. 1996. Conserved left-right asymmetry of nodal expression and alterations in murine situs inversus. *Nature* **381:** 158–161.

Lustig, K.D., K. Kroll, E. Sun, R. Ramos, H. Elmendorf, and M.W. Kirschner. 1996. A Xenopus nodal-related gene that acts in synergy with noggin to induce complete secondary axis and notochord formation. *Development* **122:** 3275–3282.

Melloy, P.G., J.L. Ewart, M.F. Cohen, M.E. Desmond, M.R. Kuehn, and C.W. Lo. 1998. No turning, a mouse mutation causing left-right and axial patterning defects. *Dev. Biol.* **193:** 77–89.

Meno, C., Y. Saijoh, H. Fujii, M. Ikeda, T. Yokoyama, M. Yokoyama, Y. Toyoda, and H. Hamada. 1996. Left-right asymmetric expression of the TGF beta-family member lefty in mouse embryos. *Nature* **381:** 151–155.

Meno, C., Y. Ito, Y. Saijoh, Y. Matsuda, K. Tashiro, S. Kuhara, and H. Hamada. 1997. Two closely-related left-right asymmetrically expressed genes, lefty-1 and lefty-2: Their distinct expression domains, chromosomal linkage and direct neuralizing activity in Xenopus embryos. *Genes Cells* **2:** 513–524.

Meno, C., A. Shimono, Y. Saijoh, K. Yashiro, K. Mochida, S. Ohishi, S. Noji, H. Kondoh, and H. Hamada. 1998. lefty-1 is required for left-right determination as a regulator of lefty-2 and nodal. *Cell* **94:** 287–297.

Meno, C., K. Gritsman, S. Ohishi, Y. Ohfuji, E. Heckscher, K. Mochida, A. Shimono, H. Kondoh, W.S. Talbot, E.J. Robertson et al. 1999. Mouse *Lefty-2* and zebrafish *antivin* are feed-

back inhibitors of *Nodal* signaling during vertebrate gastrulation. *Mol. Cell* (in press).
Meyers, E.N. and G.R. Martin. 1999. Differences in left-right axis pathways in mouse and chick: Functions of FGF8 and SHH. *Science* **285:** 403–406.
Milewski, W.M., S.J. Duguay, S.J. Chan, and D.F. Steiner. 1998. Conservation of PDX-1 structure, function, and expression in zebrafish. *Endocrinology* **139:** 1440–1449.
Mortensen, R. 1999. Gene targeting by homologous recombination. In *Current protocols in molecular biology* (ed. F.M. Ausubel, R. Brent, R.E. Kingston, D.D. Moore, J.G. Seidman, J.A. Smith, and K. Struhl), pp. 9.15.11–19.17.13. John Wiley & Sons, New York, NY.
New, H.V., A.L. Kavka, J.C. Smith, and J.B. Green. 1997. Differential effects on Xenopus development of interference with type IIA and type IIB activin receptors. *Mech Dev.* **61:** 175–186.
Nomura, M. and E. Li. 1998. Smad2 role in mesoderm formation, left-right patterning and craniofacial development. *Nature* **393:** 786–790.
Oh, S.P. and E. Li. 1997. The signaling pathway mediated by the type IIB activin receptor controls axial patterning and lateral asymmetry in the mouse. *Genes & Dev.* **11:** 1812–1826.
Pagan-Westphal, S.M. and C.J. Tabin. 1998. The transfer of left-right positional information during chick embryogenesis. *Cell* **93:** 25–35.
Piedra, M.E., J.M. Icardo, M. Albajar, J.C. Rodriguez-Rey, and M.A. Ros. 1998. Pitx2 participates in the late phase of the pathway controlling left-right asymmetry. *Cell* **94:** 319–324.
Ramsdell, A.F. and H.J. Yost. 1998. Molecular mechanisms of vertebrate left-right development. *Trends Genet.* **14:** 459–465.
Rebagliati, M.R., R. Toyama, C. Fricke, P. Haffter, and I.B. Dawid. 1998. Zebrafish nodal-related genes are implicated in axial patterning and establishing left-right asymmetry. *Dev. Biol.* **199:** 261–272.
Ryan, A.K., B. Blumberg, C. Rodriguez-Esteban, S. Yonei-Tamura, K. Tamura, T. Tsukui, J. de la Pena, W. Sabbagh, J. Greenwald, S. Choe et al. 1998. Pitx2 determines left-right asymmetry of internal organs in vertebrates. *Nature* **394:** 545–551.
Sampath, K., A.M. Cheng, A. Frisch, and C.V. Wright. 1997. Functional differences among Xenopus nodal-related genes in left-right axis determination. *Development* **124:** 3293–3302.
Schier, A.F., S.C.F. Neuhauss, K.A. Helde, W.S. Talbot, and W. Driever. 1997. The *one-eyed pinhead* gene functions in mesoderm and endoderm formation in zebrafish and interacts with *no tail*. *Development* **124:** 327–342.
Serbedzija, G.N., J.N. Chen, and M.C. Fishman. 1998. Regulation in the heart field of zebrafish. *Development* **125:** 1095–1101.
Shen, M.M., H. Wang, and P. Leder. 1997. A differential display strategy identifies *Cryptic*, a novel EGF-related gene expressed in the axial and lateral mesoderm during mouse gastrulation. *Development* **124:** 429–442.
Thisse, C. and B. Thisse. 1999. Antivin, a novel and divergent member of the TGFbeta superfamily, negatively regulates mesoderm induction. *Development* **126:** 229–240.
Waldrip, W.R., E.K. Bikoff, P.A. Hoodless, J.L. Wrana, and E.J. Robertson. 1998. Smad2 signaling in extraembryonic tissues determines anterior-posterior polarity of the early mouse embryo. *Cell* **92:** 797–808.
Weinstein, M., X. Yang, C. Li, X. Xu, J. Gotay, and C.X. Deng. 1998. Failure of egg cylinder elongation and mesoderm induction in mouse embryos lacking the tumor suppressor smad2. *Proc. Natl. Acad. Sci.* **95:** 9378–9383.
Yoshioka, H., C. Meno, K. Koshiba, M. Sugihara, H. Itoh, Y. Ishimaru, T. Inoue, H. Ohuchi, E.V. Semina, J.C. Murray et al. 1998. Pitx2, a bicoid-type homeobox gene, is involved in a lefty-signaling pathway in determination of left-right asymmetry. *Cell* **94:** 299–305.
Zhang, J., W.S. Talbot, and A.F. Schier. 1998. Positional cloning identifies zebrafish *one-eyed pinhead* as a permissive EGF-related ligand required during gastrulation. *Cell* **92:** 241–251.